Применение методов машинного обучения для голографических моделей КХД

Павел Слепов
Совместно с И.Я. Арефьевой, А. Николаевым, М. Храмцовым

Математический институт им. В.А. Стеклова Российской академии наук

Сессия-конференция СЯФ ОФН РАН, г. Новосибирск

13.03.2026

Studies of QCD Phase Diagram is the main goal of new facilities

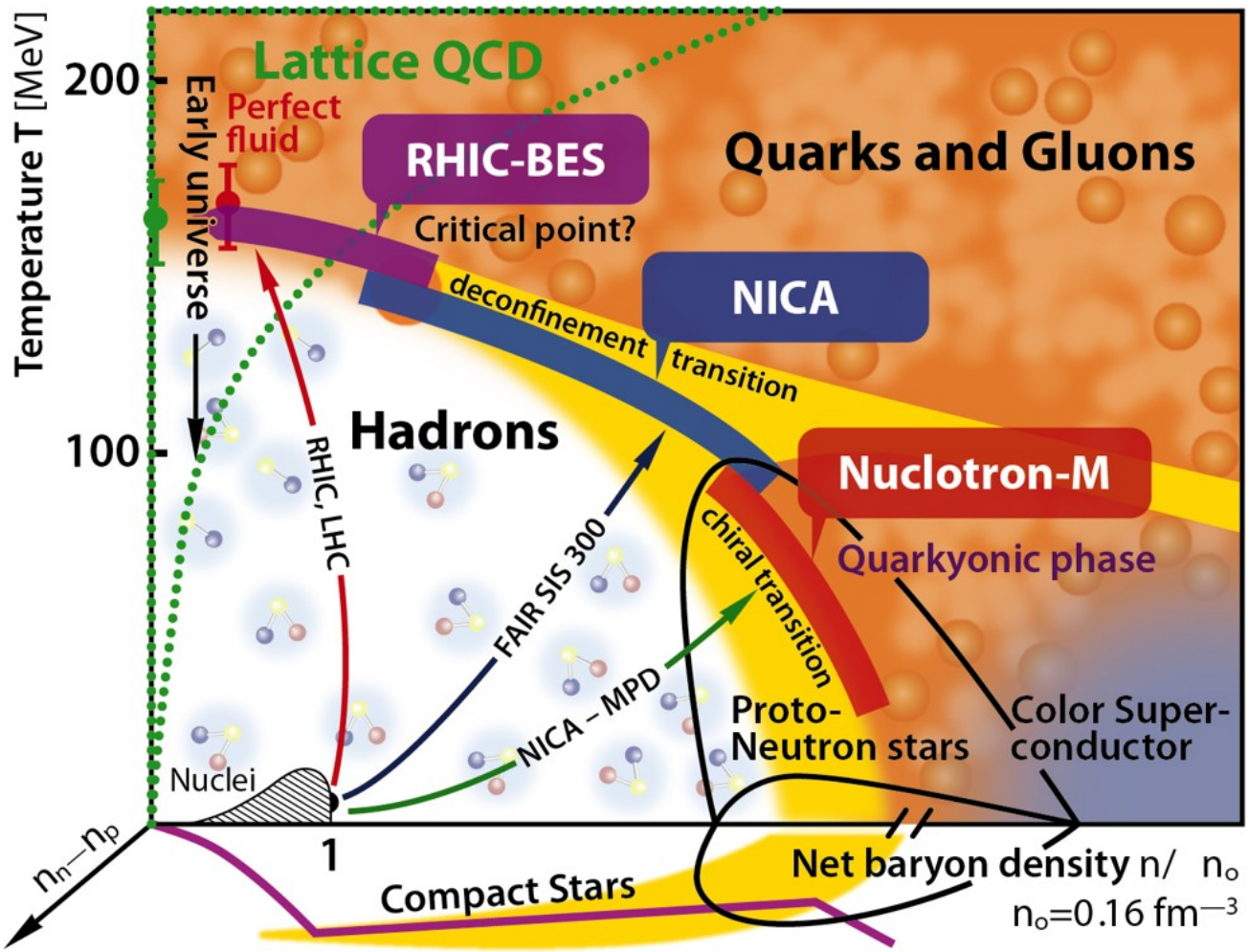

From: https://nica.jinr.ru/physics.php

Holographic QCD phase diagram for light quarks

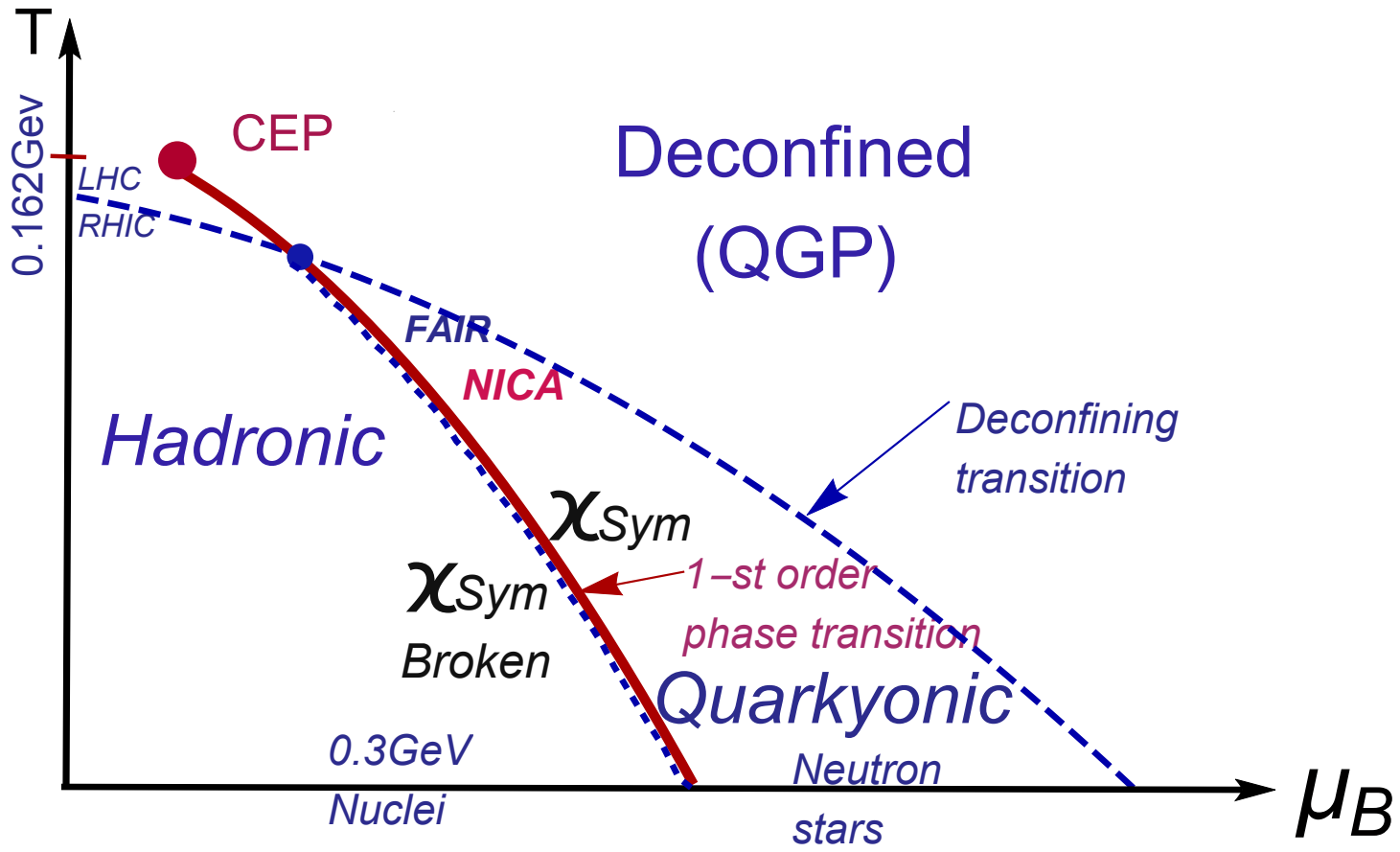

Motivation

Purpose: Study of the QCD phase diagram in (μ,T) plane for the fully anisotropic background

Multiplicity $\mathcal{M} \propto s_{AdS}^{0.33}$ vs $\mathcal{M} \propto s_{LHC}^{0.155}$

$\mathcal{M} \propto s^{\frac{1}{\nu+2}}$, $\nu = 4.5$ I.Aref'eva, A.Golubtsova, JHEP **04**, 011 (2015)

Strong magnetic field at the early stages of HIC: $eB \sim 0.3 GeV^2$

QCD Phase Diagram: Lattice

Phase diagram
on quark mass

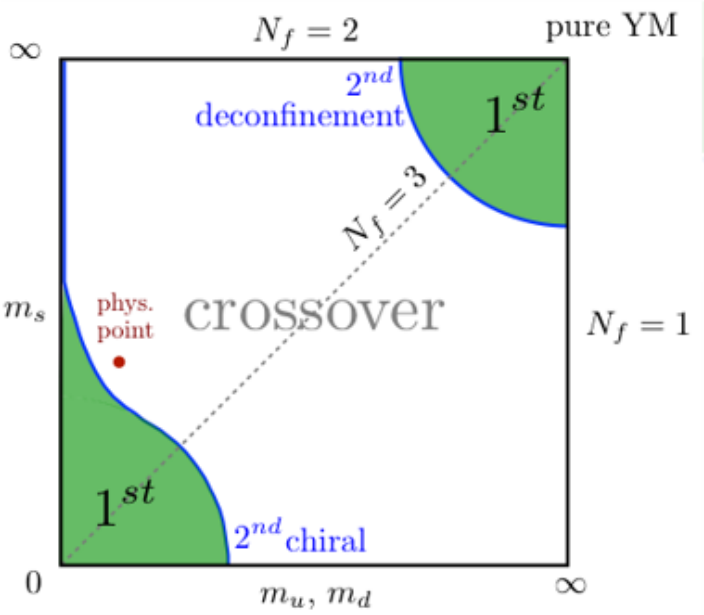

Columbia plot
Brown et al., PRL (1990)

Main problem with $\mu \neq 0$
Imaginary chemical potential method

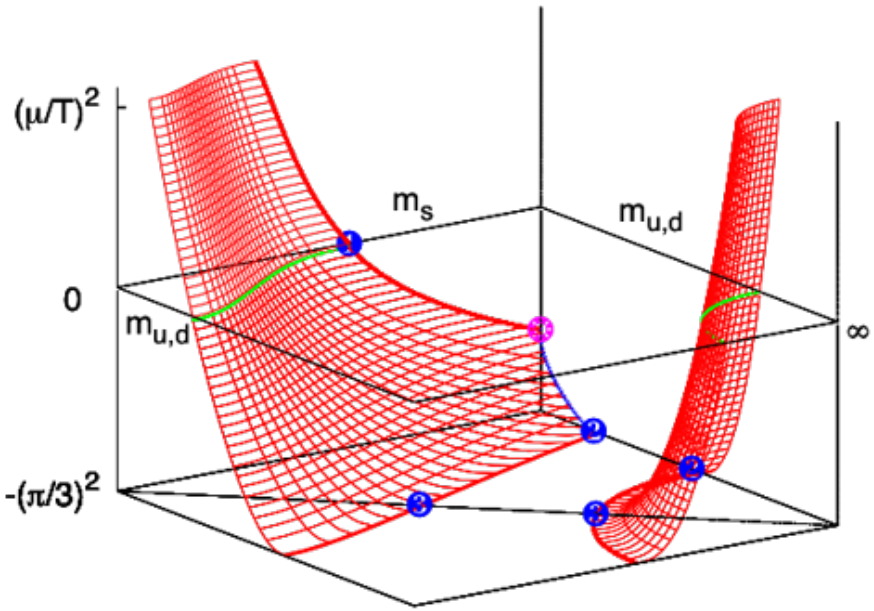

Philipsen, Pinke, PRD (2016)

"Light" and "Heavy" Quarks from Columbia Plot

Light quarks

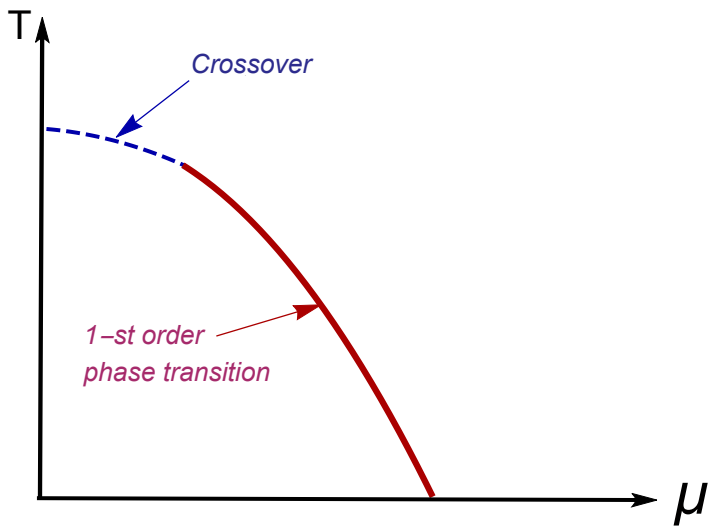

Heavy quarks

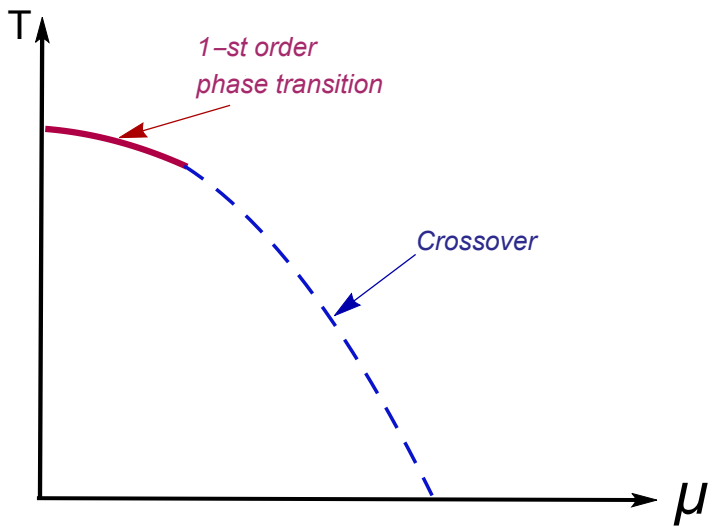

Temperature as function of horizon for different μ in isotropic models for light and heavy quarks

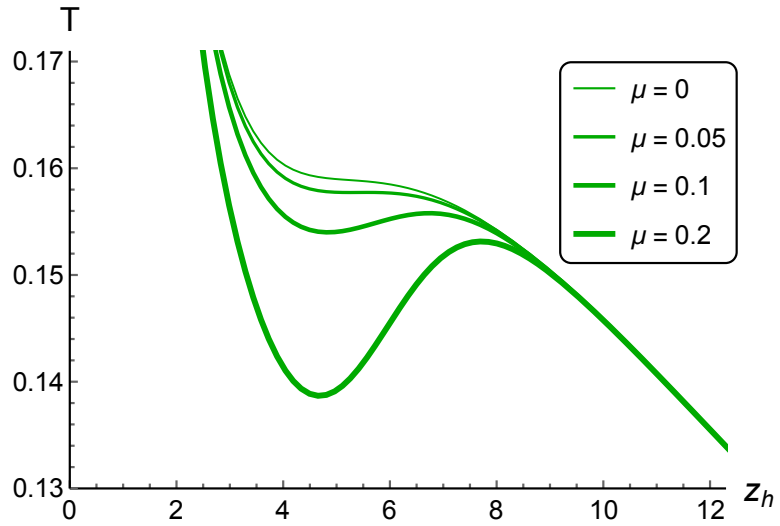

Light Quarks $b(z) = e^{-2\,a\,\ln(bz^2+1)}$

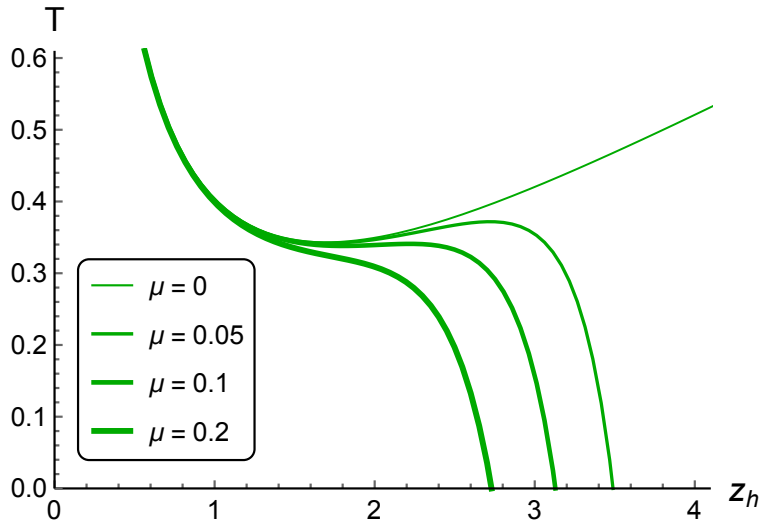

Heavy Quarks $b(z) = e^{-cz^2/4}$

The main question to discuss is: what directly measurable quantities indicate the phase transition structure?

- Jet Quenching – I. Y. Aref'eva, A. Hajilou, A. Nikolaev and P. S., "Jet quenching in holographic QCD as an indicator of phase transitions in anisotropic regimes," PRD **112** (2025) 126007
- Energy loss – I. Y. Aref'eva, A. Hajilou, K. Rannu and P. S., "Spatial Wilson Loops and Energy Loss for Heavy Quarks...," [arXiv:2601.09611 [hep-th]].
- Direct photons – I.Ya. Aref'eva, A. Ermakov and P. S., "Direct photons emission rate ... with first-order phase transition," EPJC **82** (2022) 85
- Cross-sections – I.Ya.Aref'eva, A. Hajilou, P. S. and M. Usova, "Running coupling for HQCD...: Isotropic case," PRD **110** (2024) 126009
  I.Ya. Aref'eva, A. Hajilou, A. Nikolaev and P. S., "HQCD running coupling ... in strong magnetic field," PRD **110** (2024) 086021

Holographic model of an anisotropic plasma in a magnetic field at a non-zero chemical potential

I.Aref'eva, K.Rannu'18; I Aref'eva, K. Rannu, P.S.'21

$$S=\int d^5x\,\sqrt{-g}\left[R-\frac{f_1(\phi)}{4}F^2_{(1)}-\frac{f_2(\phi)}{4}F^2_{(2)}-\frac{f_B(\phi)}{4}F^2_{(B)}-\frac{1}{2}\partial_M\phi\partial^M\phi-V(\phi)\right]$$

$$ds^2=\frac{L^2}{z^2}\mathfrak{b}(z)\left[-g(z)\,dt^2+dx^2+\left(\frac{z}{L}\right)^{2-\frac{2}{\nu}}dy_1^2+e^{c_B z^2}\left(\frac{z}{L}\right)^{2-\frac{2}{\nu}}dy_2^2+\frac{dz^2}{g(z)}\right]$$

$$A_{(1)\mu}=A_t(z)\delta^0_\mu \qquad A_t(0)=\mu \qquad F_{(2)}=q_2\,dy^1\wedge dy^2 \qquad F_{(B)}=q_B\,dx\wedge dy^1$$

Giataganas'13; Aref'eva, Golubtsova'14; Gürsoy, Järvinen '19; Dudal et al.'19

$\mathfrak{b}(z)=e^{2\mathcal{A}(z)}$ $\Leftrightarrow$ quarks mass

"Bottom-up approach"

Heavy quarks (c, b):

$\mathcal{A}(z)=-\,cz^2/4$ — *Andreev, Zakharov'06*

$\mathcal{A}(z)=-\,cz^2/4-(p-c_B\,q_3)z^4$ — *Aref'eva, Hajilou, Rannu, P.S.' 23*

Light quarks (u, d, s)

$\mathcal{A}(z)=-\,a\ln(bz^2+1)$ — *Li, Yang, Yuan'17*

$\mathcal{A}(z)=-\,d\ln((az^2+1)(bz^4+1))$ — *Zhu, Chen, Zhou, Zhang, Huang'25*

Boundary conditions

$$A_t(0) = \mu, \quad A_t(z_h) = 0,$$
$$g(0) = 1, \quad g(z_h) = 0,$$
$$\phi(z_0) = 0.$$

Boundary condition for dilaton field

Holographic running coupling $\alpha(z) = e^{\varphi(z)}$

$\varphi(z)$ - dilaton field $\varphi(z)$ is defined up to a constant: $\varphi(z)\Big|_{z=z_0} = 0.$

There are 3 choices: a) $z_0 = 0$ b) $z_0 = f(z_h)$ c) $z_0 = z_h$

Light Quark Model: $z_0 = 10\exp(-z_h/4) + 0.1$

I Aref'eva, K.Rannu, P.S., JHEP'21

With this boundary condition the temperature dependence of σ_s fits the known lattice data

Cordaso, Bicudo 1111.1317

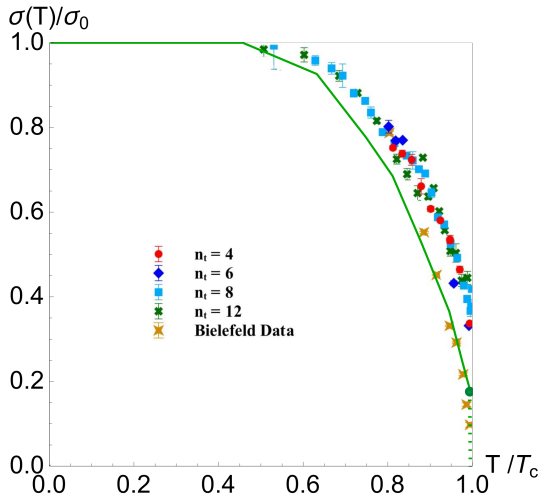

Heavy Quark Model: $z_0 = \exp(-z_h/4) + 0.1$

I.Ya.Aref'eva, A. Hajilou, P. S. and M. Usova, PRD'24

1-st order phase transition for “light” and “heavy” quarks in Holography

Light quarks

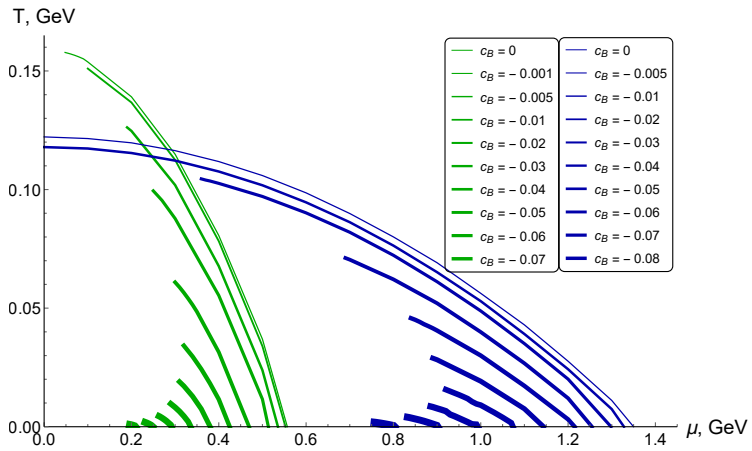

Aref’eva, Ermakov, Rannu, P.S.,EPJC’23

Heavy quarks

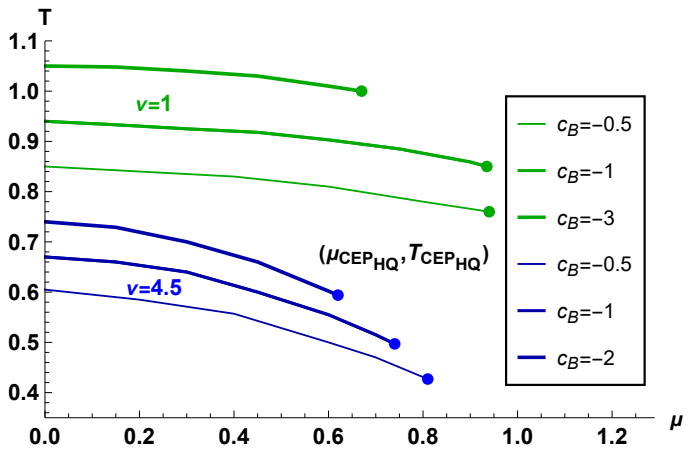

Aref’eva, Hajilou, Rannu, P.S.,EPJC’23

1-st order phase transition for "light" and "heavy" quarks in Holography

Light quarks

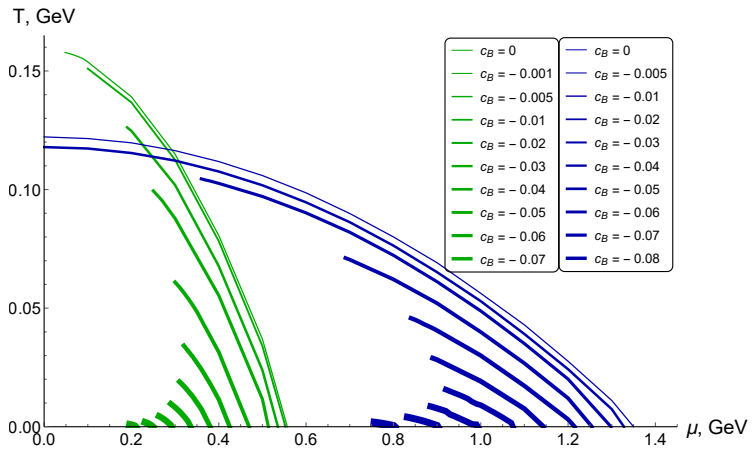

Aref'eva, Ermakov, Rannu, P.S.,EPJC'23

Heavy quarks

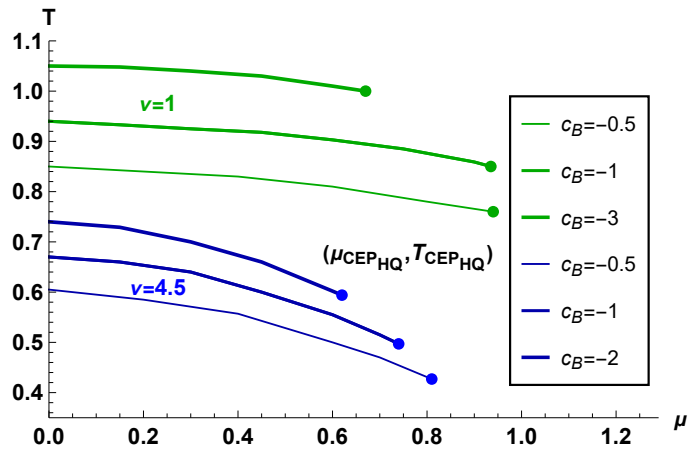

Aref'eva, Hajilou, Rannu, P.S.,EPJC'23

- QCD Phase Diagram from Lattice Columbia plot
  Brown et al.'90 Philipsen, Pinke'16
- **Main problem on Lattice:** $\mu \neq 0$

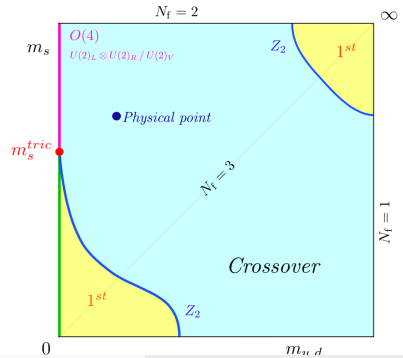

3 types of Wilson loops in quantum gauge theories!

- **Time-like loop** $\mathcal{C} = t \times x, \quad t, x >> \ell_{QCD}$
  $\ell_{QCD} \sim \frac{\hbar c}{\Lambda} \approx 1\text{fm}, W_F[C] \underset{\substack{t\to\infty \\ x\to\infty}}{\sim} e^{-\sigma_{st} t x}$
- **Space-like loop** $\mathcal{C} = x_1 \times x_2, \quad x_i >> \ell_{QCD}$

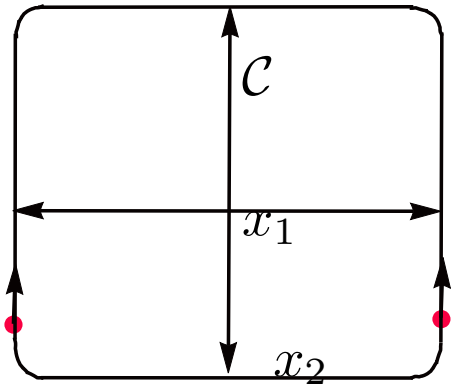

$$W_F[C] \underset{\substack{x_1\to\infty \\ x_2\to\infty}}{\sim} e^{-\sigma_{DF} x_1 x_2}$$

σ_{DF} **drag force parameter**, related with energy loss

- **Light-like loop** $\mathcal{C} = x_- \times x_2, \quad x_- >> x_2$

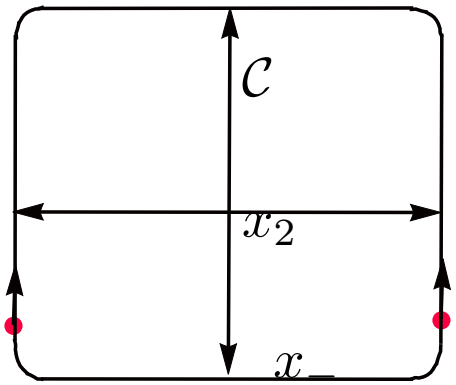

$$W_{Ad}[C] \underset{\substack{x_-\to\infty \\ x_2\to 0}}{\sim} e^{-q\, x_- x_2^2}$$

q - jet quenching parameter

the average transverse momentum squared transferred from the parton to the medium per unit path length

3 types of Wilson loops in quantum gauge theories!

- **Time-like loop** $\mathcal{C} = t \times x, \quad t, x >> \ell_{QCD}$
  $\ell_{QCD} \sim \frac{\hbar c}{\Lambda} \approx 1\text{fm}, W_F[C] \underset{\substack{t\to\infty \\ x\to\infty}}{\sim} e^{-\sigma_{st} t x}$

- **Space-like loop** $\mathcal{C} = x_1 \times x_2, \quad x_i >> \ell_{QCD}$

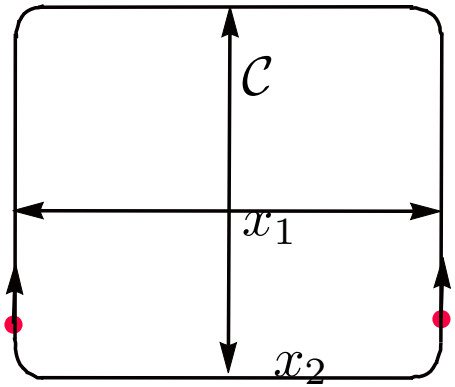

$$W_F[C] \underset{\substack{x_1\to\infty \\ x_2\to\infty}}{\sim} e^{-\sigma_{DF} x_1 x_2}$$

σ_{DF} **drag force parameter**, related with energy loss

- **Light-like loop** $\mathcal{C} = x_- \times x_2, \quad x_- >> x_2$

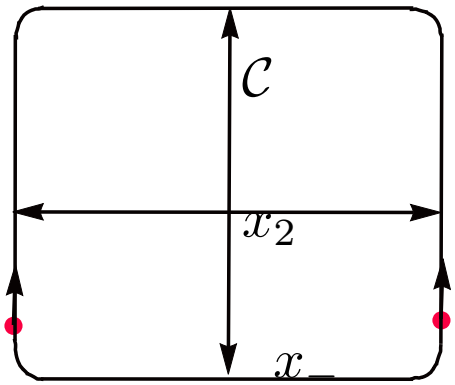

$$W_{Ad}[C] \underset{\substack{x_-\to\infty \\ x_2\to 0}}{\sim} e^{-q\, x_- x_2^2}$$

q **- jet quenching parameter**

the average transverse momentum squared transferred from the parton to the medium per unit path length

- Wilson Loops in holographic QCD
  J. Maldacena'98

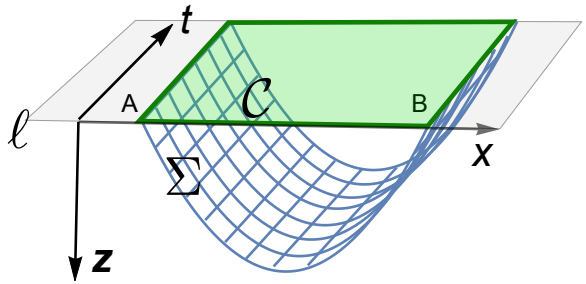

- String action "on a barn"

$$S_{NG} = \int d\tau d\xi\, M(z(\xi)) \sqrt{\mathcal{F}(z(\xi)) + (z'(\xi))^2}$$

H.Liu, K.Rajagopal, U.Wiedemann'06 Conf. case: $q \sim T^3$

Jet quenching for non-zero magnetic field and initial anisotropy. Analytical formula & Numerical results

$$q_i(z_h,\mu,c_B,\nu)=\frac{L^2}{\pi\alpha' a_i}\sim\frac{1}{a_i},\quad i=2,3$$

$$a_2=\int_0^{z_h}\frac{e^{-2\mathcal{A}_s(z)}\left(\frac{z}{L}\right)^{2/\nu}}{\sqrt{g(z)(1-g(z))}}dz\qquad a_3=\int_0^{z_h}\frac{e^{-2\mathcal{A}_s(z)-c_B z^2}\left(\frac{z}{L}\right)^{2/\nu}}{\sqrt{g(z)(1-g(z))}}dz$$

$$g(z,z_h,\mu,c_B,\nu)=e^{c_B z^2}\left[1-\frac{I_1(z)}{I_1(z_h)}+\frac{\mu^2\left(2c-c_B\right)I_2(z)}{L^2\left(1-e^{(2c-c_B)z_h^2/2}\right)^2}\left(1-\frac{I_1(z)I_2(z_h)}{I_1(z_h)I_2(z)}\right)\right]$$

$$I_1(z)=\int_0^z\left(1+b\chi^2\right)^{3a}\frac{\chi^{1+\frac{2}{\nu}}}{e^{\frac{3}{2}c_B\chi^2}}d\chi,\qquad I_2(z)=\int_0^z\left(1+b\chi^2\right)^{3a}\frac{\chi^{1+\frac{2}{\nu}}}{e^{(-c+2c_B)\chi^2}}d\chi$$

$$T=\frac{|g'|}{4\pi}\Big|_{z=z_h}\qquad s=\left(\frac{L}{z_h}\right)^{1+\frac{2}{\nu}}\frac{e^{c_B z_h^2/2}\left(1+bz_h^2\right)^{-3a}}{4}\qquad F=\int_{z_h}^{z_{h_2}}s\,dT=\int_{z_h}^{z_{h_2}}s\,T'dz$$

Jet quenching for $c_B = -0.05$ and $\nu = 1$ for LQ model. Numerical results for a_2 and a_3

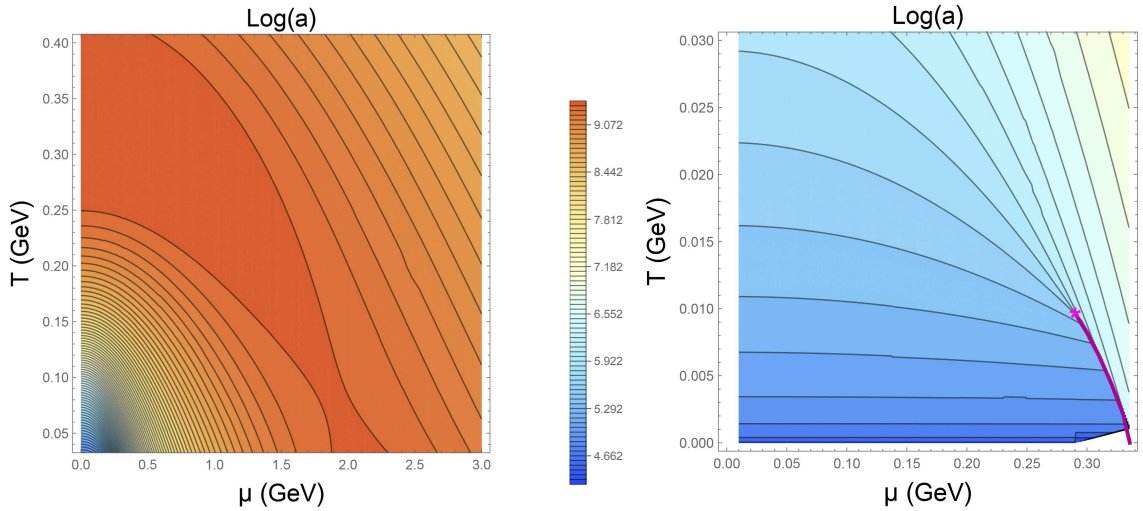

a_2 orientation

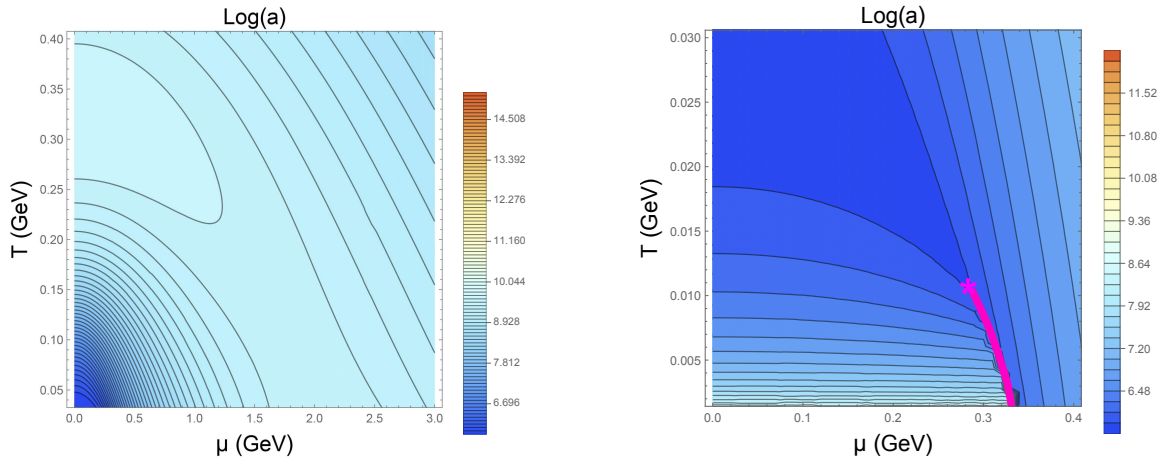

a_3 orientation

String tension for SWLs vs drag forces

For solution $\mathfrak{g}_1 = 1$, $\mathfrak{g}_2 = (z/L)^{2-2/\nu}$, $\mathfrak{g}_3 = (z/L)^{2-2/\nu} e^{c_B z^2}$:

$$\sigma_{xY_1} = \sigma_{Xy_1} = \left(\frac{L^2 b_s(z)}{z^2}\right) \sqrt{\mathfrak{g}_1 \mathfrak{g}_2} = \left(\frac{L^{1+1/\nu} b_s(z)}{z^{1+1/\nu}}\right),$$

$$\sigma_{xY_2} = \left(\frac{L^2 b_s(z)}{z^2}\right) \sqrt{\mathfrak{g}_1 \mathfrak{g}_3} = \left(\frac{L^{1+1/\nu} b_s(z)}{z^{1+1/\nu}}\right) e^{c_B z^2/2},$$

$$\sigma_{y_1 Y_2} = \left(\frac{L^2 b_s(z)}{z^2}\right) \sqrt{\mathfrak{g}_2 \mathfrak{g}_3} = \left(\frac{L^{2/\nu} b_s(z)}{z^{2/\nu}}\right) e^{c_B z^2/2},$$

where $z = z_h$ or $z = z_{DW}$ (if the DW exists).

String tension for SWLs vs drag forces

For solution $\mathfrak{g}_1 = 1$, $\mathfrak{g}_2 = (z/L)^{2-2/\nu}$, $\mathfrak{g}_3 = (z/L)^{2-2/\nu} e^{c_B z^2}$:

$$\sigma_{xY_1} = \sigma_{Xy_1} = \left(\frac{L^2 b_s(z)}{z^2}\right) \sqrt{\mathfrak{g}_1 \mathfrak{g}_2} = \left(\frac{L^{1+1/\nu} b_s(z)}{z^{1+1/\nu}}\right),$$

$$\sigma_{xY_2} = \left(\frac{L^2 b_s(z)}{z^2}\right) \sqrt{\mathfrak{g}_1 \mathfrak{g}_3} = \left(\frac{L^{1+1/\nu} b_s(z)}{z^{1+1/\nu}}\right) e^{c_B z^2/2},$$

$$\sigma_{y_1 Y_2} = \left(\frac{L^2 b_s(z)}{z^2}\right) \sqrt{\mathfrak{g}_2 \mathfrak{g}_3} = \left(\frac{L^{2/\nu} b_s(z)}{z^{2/\nu}}\right) e^{c_B z^2/2},$$

where $z = z_h$ or $z = z_{DW}$ (if the DW exists). The answers can be compared with drag forces I. Aref'eva Phys.Part.Nucl. **51** 4, 489-496 (2020), O. Andreev, Mod. Phys. Lett. A **33**, 06 (2018), S. J. Sin and I. Zahed, Phys.Lett. B **648**, 318 (2007).

String tension for SWLs vs drag forces

For solution $\mathfrak{g}_1 = 1$, $\mathfrak{g}_2 = (z/L)^{2-2/\nu}$, $\mathfrak{g}_3 = (z/L)^{2-2/\nu} e^{c_B z^2}$:

$$\sigma_{xY_1} = \sigma_{Xy_1} = \left(\frac{L^2 b_s(z)}{z^2}\right) \sqrt{\mathfrak{g}_1 \mathfrak{g}_2} = \left(\frac{L^{1+1/\nu} b_s(z)}{z^{1+1/\nu}}\right),$$

$$\sigma_{xY_2} = \left(\frac{L^2 b_s(z)}{z^2}\right) \sqrt{\mathfrak{g}_1 \mathfrak{g}_3} = \left(\frac{L^{1+1/\nu} b_s(z)}{z^{1+1/\nu}}\right) e^{c_B z^2/2},$$

$$\sigma_{y_1 Y_2} = \left(\frac{L^2 b_s(z)}{z^2}\right) \sqrt{\mathfrak{g}_2 \mathfrak{g}_3} = \left(\frac{L^{2/\nu} b_s(z)}{z^{2/\nu}}\right) e^{c_B z^2/2},$$

where $z = z_h$ or $z = z_{DW}$ (if the DW exists). The answers can be compared with drag forces

I. Aref'eva Phys.Part.Nucl. **51** 4, 489-496 (2020),
O. Andreev, Mod. Phys. Lett. A **33**, 06 (2018),
S. J. Sin and I. Zahed, Phys.Lett. B **648**, 318 (2007).

The drag forces for metric with $\mathfrak{g}_1 = 1$:

$$p_x = v_x \frac{b_s(z)}{z^2} \qquad p_{y_1} = v_{y_1} \frac{b_s(z)}{z^2} \mathfrak{g}_2(z) \qquad p_{y_2} = v_{y_2} \frac{b_s(z)}{z^2} \mathfrak{g}_3(z), \tag{1}$$

$v_x = v\sqrt{\mathfrak{g}_2}$, $v_{y_1} = v\frac{\sqrt{\mathfrak{g}_3}}{\mathfrak{g}_2}$, $v_{y_2} = v\frac{\sqrt{\mathfrak{g}_2}}{\sqrt{\mathfrak{g}_3}}$ with some constant v

Phase transitions of $\mathcal{V}_1$ for $\nu = 1,\ 4.5$ in magnetic catalysis model with modified warp-factor

Modified Warp-factor: $\mathcal{A}(z) = -cz^2/4 - (p - c_B\, q_3)z^4$

Aref'eva, Hajilou, Rannu and P. S., Eur. Phys. J. C 83, 12, 1143 (2023)

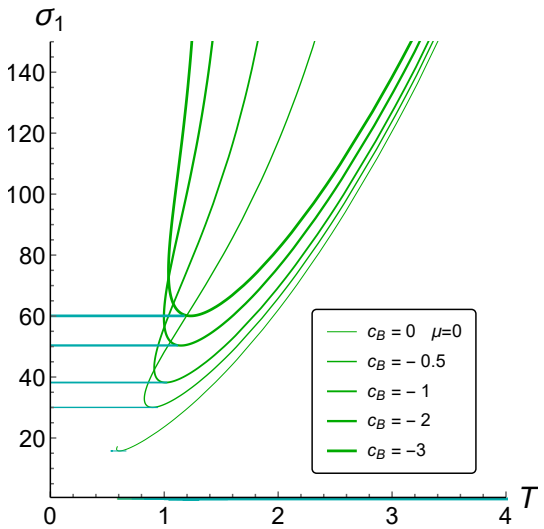

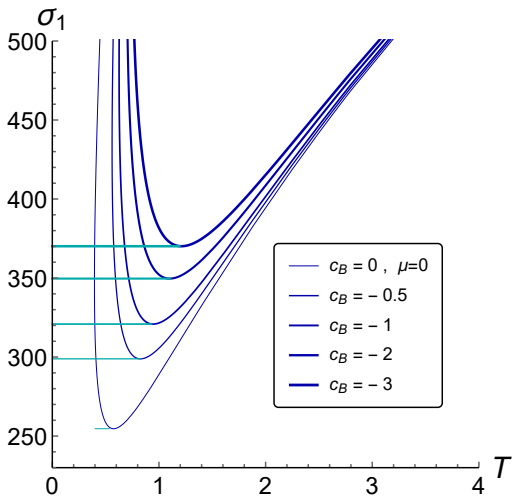

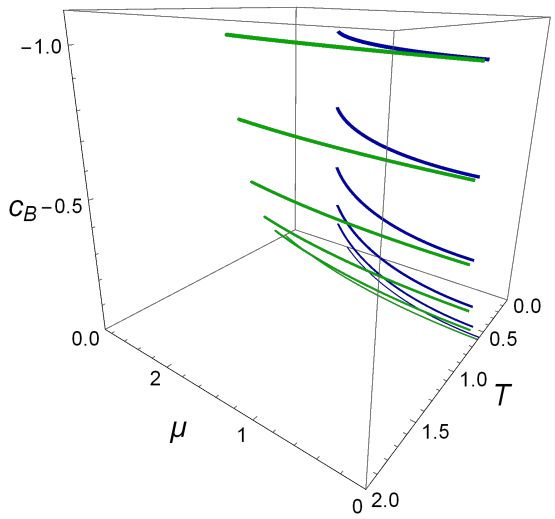

Phase diagrams for SWL in (μ, T)-plane

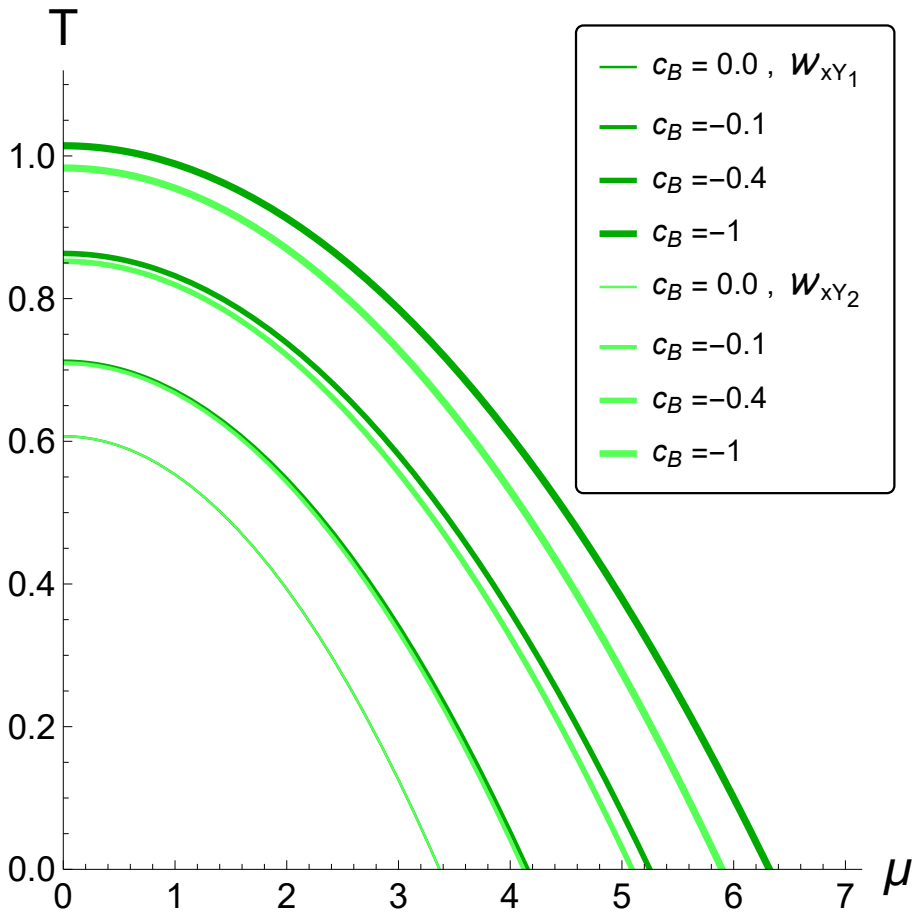

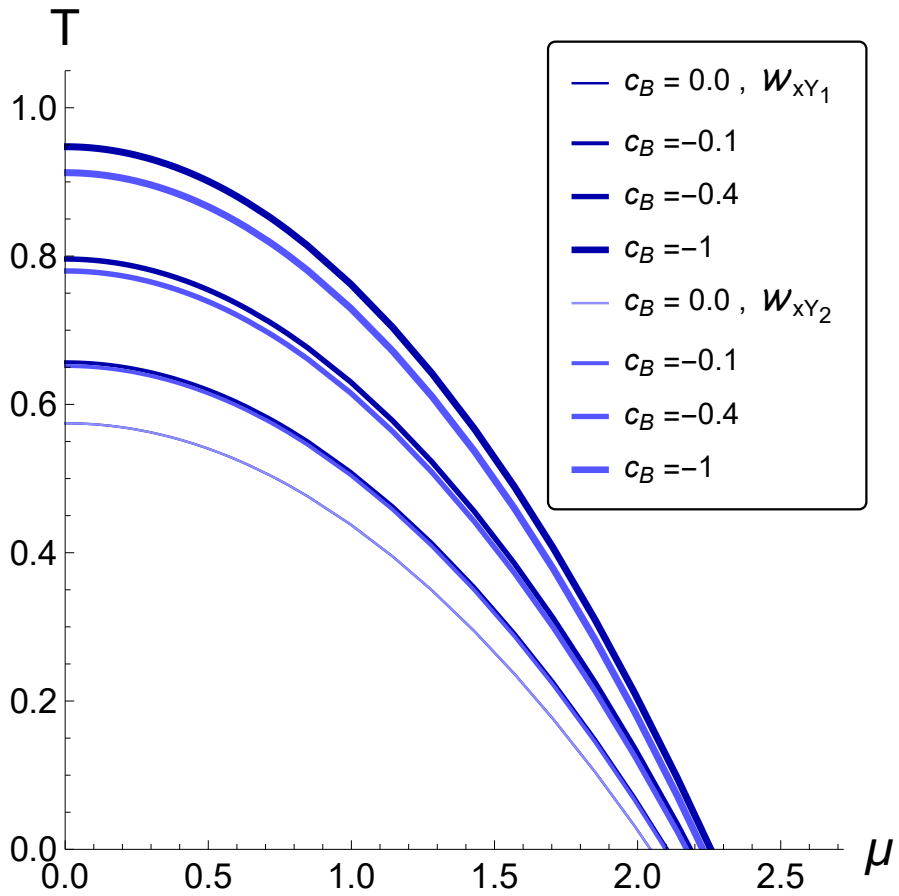

Spatial string tension σ_2 dependence on temperature

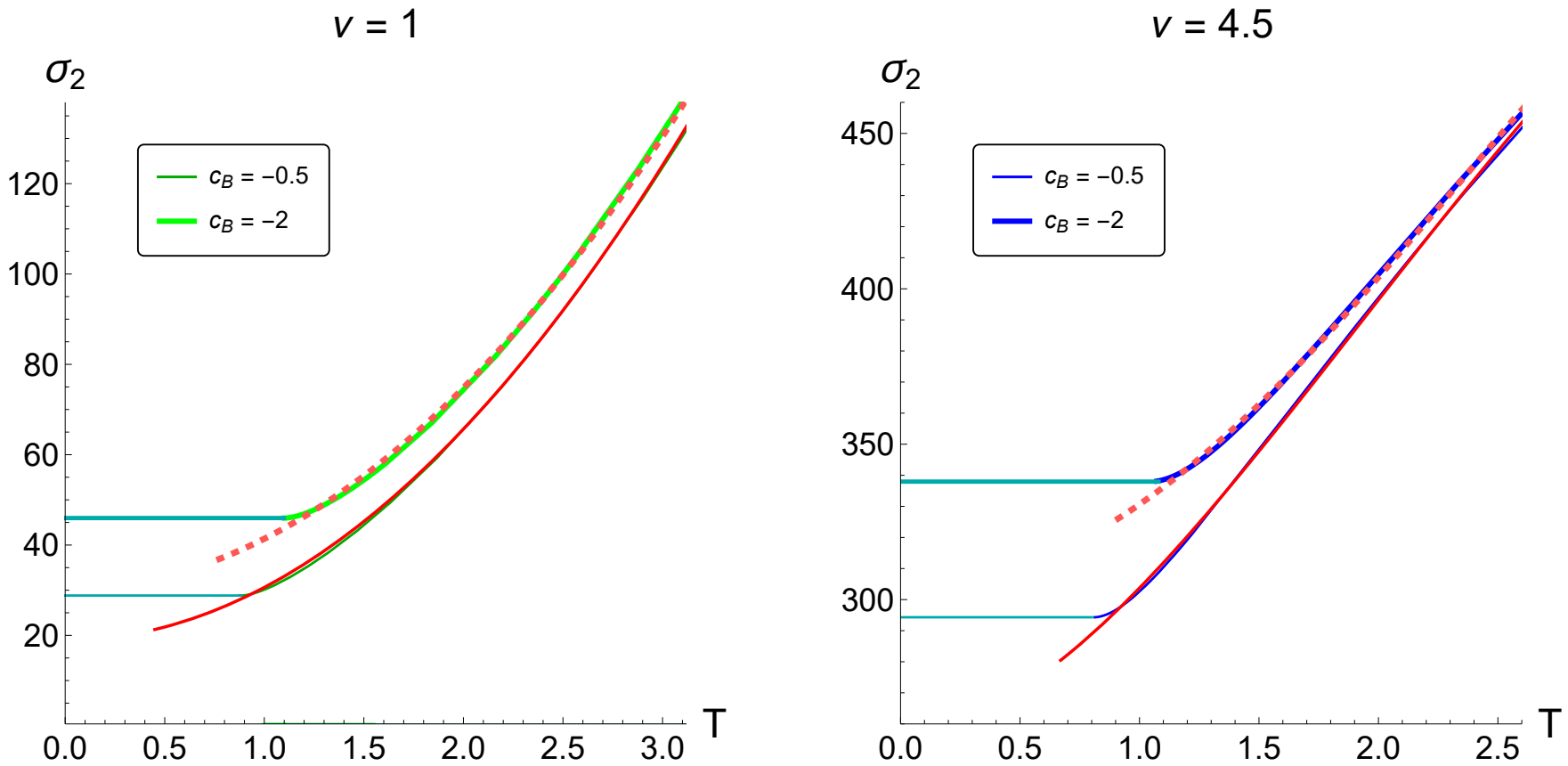

Spatial string tension σ_2 in the second orientation $\mathcal{W}_{xY_2}$ as a function of temperature T at $\mu = 0$ for isotropic case $\nu = 1$ that the solid red curve is $18.9 + 11.7\,T^2$, the dashed red curve is $30.2 + 11.1\,T^2$, and for anisotropic case $\nu = 4.5$ the solid red curve is $258.3 + 58.1\,T^2 - 13.6\,T^3 + 0.9\,T^4$, and the dashed red curve is $303.6 + 26.7\,T^2 + 1.3\,T^3 - 1.1\,T^4$; $[\sigma]^{\frac{1}{2}} = [T] = [\mu] = [c_B]^{\frac{1}{2}} = \text{GeV}$.

$c_B = 0$ $c_B = -0.005GeV^2$ $c_B = -0.05GeV^2$ $c_B = -0.5GeV^2$

$\nu = 1$

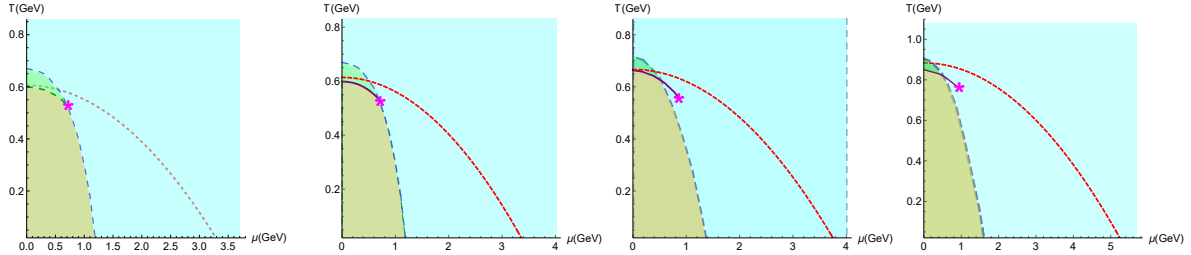

$\nu = 1.5$

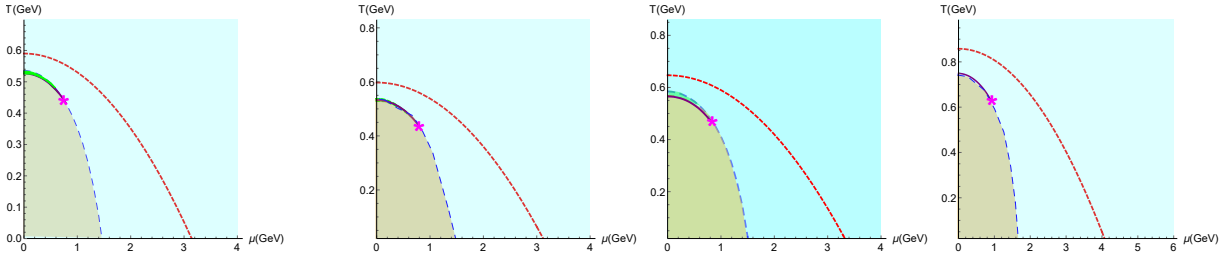

$\nu = 3$

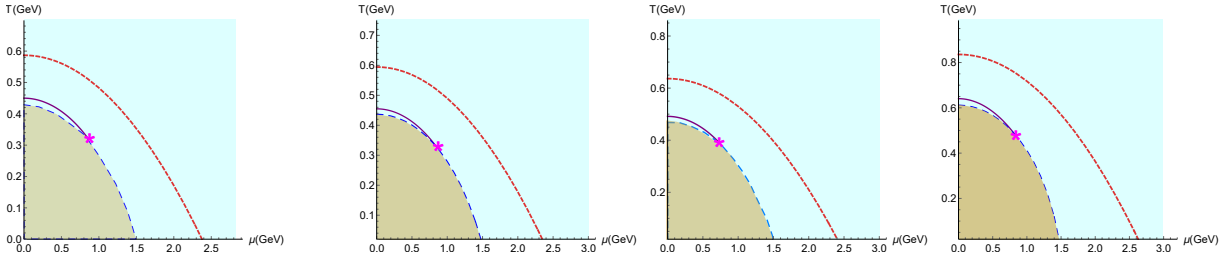

$\nu = 4.5$

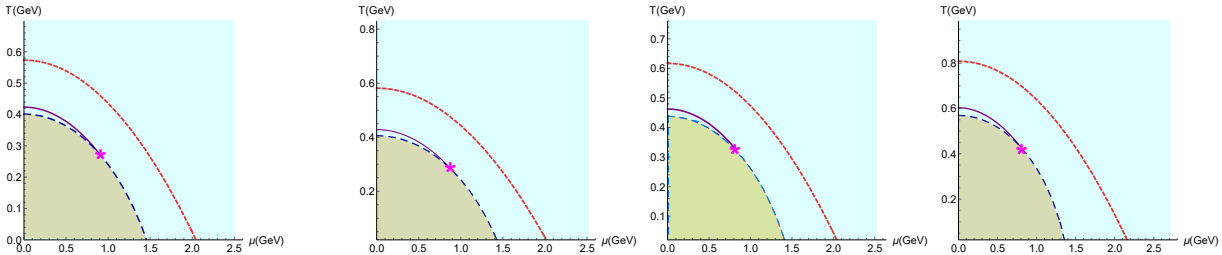

I. Y. Aref'eva, A. Hajilou, K. Rannu and P. S., 2601.09611

Machine Learning in Holographic QCD: Recent Studies

Motivation

Holographic QCD models contain bulk fields and potentials with many free parameters. Machine learning (ML) offers systematic, data-driven ways to fix these parameters and extract physical observables.

	Focus
K. Hashimoto, et al., PRD **98** (2018) 046019	Learning bulk metric from boundary correlators using deep neural network
Y. K. Yan, et al., PRD **102** (2020) 101902	Deep learning black hole metrics from shear viscosity
C. Park, et al., PRD **106** (2022) 106017	Dual geometry of entanglement entropy via deep learning
X. Chen and M. Huang, JHEP **02** (2025), 123	QCD phase diagram in EMD model & CEP with N_f flavors via deep learning

Framework: EMD Model + Machine Learning

Einstein-Maxwell-Dilaton (EMD) Holographic Model

A 5D bottom-up holographic model with action (Einstein frame):

$$S_b = \frac{1}{16\pi G_5}\int d^5x\,\sqrt{-g}\left[R - \frac{f(\phi)}{4}F^2 - \frac{1}{2}\partial_\mu\phi\,\partial^\mu\phi - V(\phi) + ...\right]$$

Analytical solutions are obtained via the **potential reconstruction method**, using the ansatz:

$$\mathcal{A}(z) = d\ln(az^2+1) + d\ln(bz^4+1) + mz^2/4 + pz^4/4 + ...$$

$$f(z) = e^{(cz^2+nz+k-A(z)+...)}$$

with free parameters $\{L,\, a,\, b,\, c,\, d,\, k,\, n,\, m,\, p,\, G_5, ...\}$.

Common Themes

- ML used to **reconstruct bulk geometry** from boundary QFT data.
- Goal: reliable **equation of state**, transport coefficients, and **phase structure** of strongly coupled QCD matter.

Holographic Models: Conventional vs. ML

Conventional Holographic model **ML Holographic model**

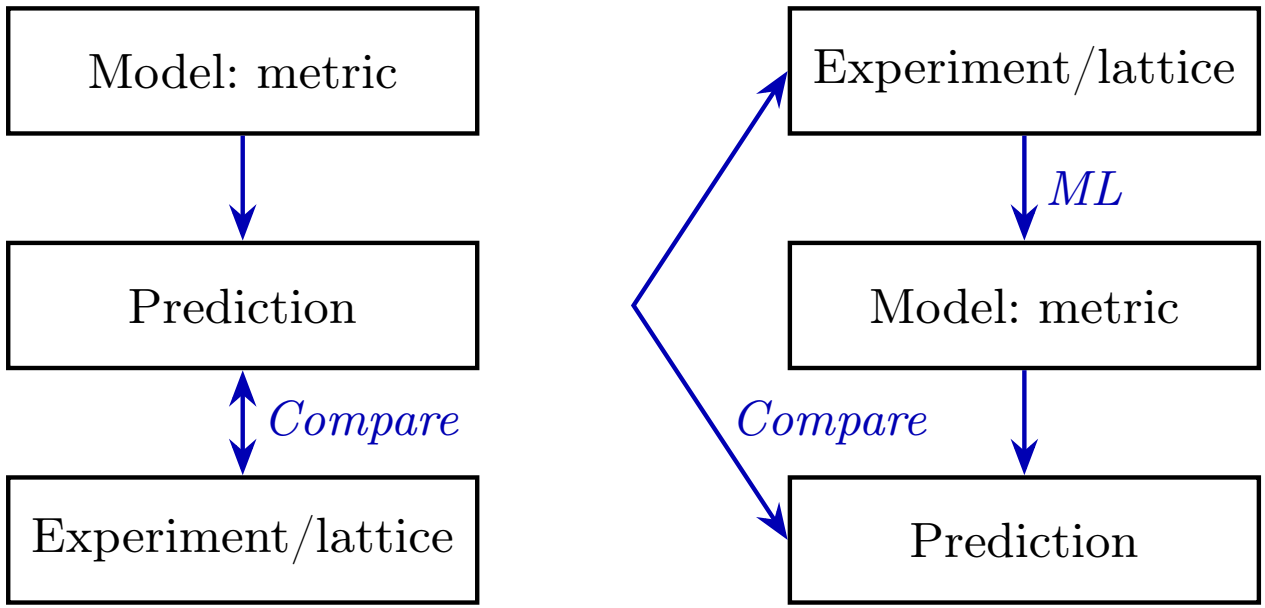

X. Chen and M. Huang, JHEP **02** (2025), 123

Flavor-Dependent CEP Locations in the T–μ_B Plane

	μ_B^c (GeV)	T^c (GeV)
$N_f = 2$	0.46	0.147
$N_f = 2+1$	0.74	0.094
$N_f = 2+1+1$	0.87	0.108

The question: What happends with confinement/deconfinement PT?

Conclusion

- The JQ parameter and string tensions (TWL, SWL) are calculated for models incorporating two types of anisotropy. Under variations of thermodynamic parameters — temperature T, chemical potential μ, and magnetic field — the string tensions and JQ parameter undergo phase transitions.

Conclusion

- The JQ parameter and string tensions (TWL, SWL) are calculated for models incorporating two types of anisotropy. Under variations of thermodynamic parameters — temperature T, chemical potential μ, and magnetic field — the string tensions and JQ parameter undergo phase transitions.
- The JQ parameter can serve as an indicator of first-order phase transitions, while the temporal Wilson loop signals the confinement/deconfinement transition, and the SWL reveals an additional phase transition.

Conclusion

- The JQ parameter and string tensions (TWL, SWL) are calculated for models incorporating two types of anisotropy. Under variations of thermodynamic parameters — temperature T, chemical potential μ, and magnetic field — the string tensions and JQ parameter undergo phase transitions.
- The JQ parameter can serve as an indicator of first-order phase transitions, while the temporal Wilson loop signals the confinement/deconfinement transition, and the SWL reveals an additional phase transition.
- Machine learning represents a powerful method for AdS/QCD models. It would therefore be of significant interest to incorporate the behavior of different Wilson loops into a unified framework using machine learning.

Conclusion

- The JQ parameter and string tensions (TWL, SWL) are calculated for models incorporating two types of anisotropy. Under variations of thermodynamic parameters — temperature T, chemical potential μ, and magnetic field — the string tensions and JQ parameter undergo phase transitions.
- The JQ parameter can serve as an indicator of first-order phase transitions, while the temporal Wilson loop signals the confinement/deconfinement transition, and the SWL reveals an additional phase transition.
- Machine learning represents a powerful method for AdS/QCD models. It would therefore be of significant interest to incorporate the behavior of different Wilson loops into a unified framework using machine learning.

What's next?
The following steps involve the selection of training data, accounting for anisotropic effects, and describing diverse datasets within a single model

Conclusion

- The JQ parameter and string tensions (TWL, SWL) are calculated for models incorporating two types of anisotropy. Under variations of thermodynamic parameters — temperature T, chemical potential μ, and magnetic field — the string tensions and JQ parameter undergo phase transitions.
- The JQ parameter can serve as an indicator of first-order phase transitions, while the temporal Wilson loop signals the confinement/deconfinement transition, and the SWL reveals an additional phase transition.
- Machine learning represents a powerful method for AdS/QCD models. It would therefore be of significant interest to incorporate the behavior of different Wilson loops into a unified framework using machine learning.

What's next?
The following steps involve the selection of training data, accounting for anisotropic effects, and describing diverse datasets within a single model

Thank you for your attention!

Backup. Light-like Wilson loops

$$ds^2 = \frac{L^2 e^{2\mathcal{A}_s}}{z^2}\left(-g(z)dt^2 + dx_1^2 + \left(\frac{z}{L}\right)^{2-2/\nu}\left(dx_2^2 + e^{c_B z^2}dx_3^2\right) + \frac{dz^2}{g(z)}\right)$$

$$dt = \frac{dx_+ + dx_-}{\sqrt{2}},\ dx_1 = \frac{dx_+ - dx_-}{\sqrt{2}}.$$

The contour $\mathcal{C}$: "short sides" with length ℓ along the x_3(or x_2) direction and the "long sides" with length L_- along the x_- direction

$$x_- = \tau; \qquad x_3(or\, x_2) = \xi$$

$$S_{NG,3} = \frac{L^2 L_-}{\pi\alpha'}\int_0^{\frac{\ell}{2}} d\xi\, \frac{e^{2A_s(z)}}{z^2}\sqrt{\frac{1-g(z)}{2}\left(e^{c_B z^2}\left(\frac{z}{L}\right)^{2-2/\nu} + \frac{z'^2}{g(z)}\right)}$$

The integral of motion

$$P = \frac{e^{2A_s(z)}(g(z)-1)}{\sqrt{2}z^2 g(z)\sqrt{(1-g(z))\left(e^{c_B z^2}\left(\frac{z}{L}\right)^{2-\frac{2}{\nu}} + \frac{z'^2}{g(z)}\right)}}$$

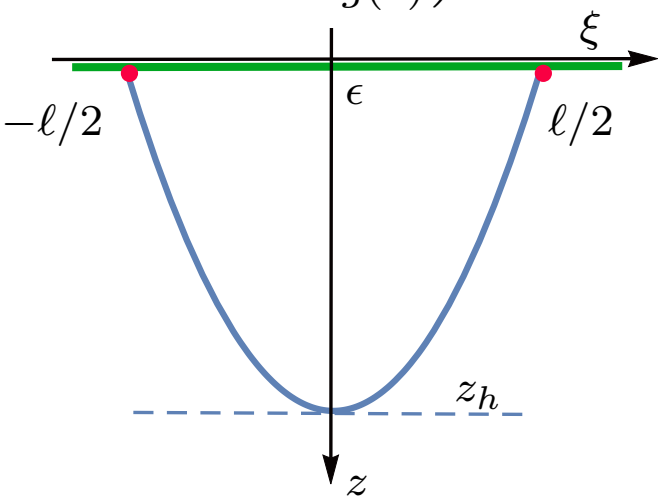

and we get for z'

$$z' = \frac{e^{2A_s + c_B z^2\left(\frac{z}{L}\right)^{-2/\nu}}}{\sqrt{2}L^2 P}\sqrt{g(1-g) - 2gL^2P^2z^2\left(\frac{z}{L}\right)^{2/\nu}e^{-4A_s - c_B z^2}}$$

Light-like Wilson loops

"Returning point":

$$g(z_*)\underbrace{\left((1-g(z_*))e^{4A_s+c_B z_*^2}-2L^2P^2z_*^2\left(\frac{z_*}{L}\right)^{2/\nu}\right)}_{\mathcal{I}}=0 \quad (*)$$

Equation (*) has two possible solutions:

$$\begin{aligned} &a) \quad g(z_*)=0, \quad \text{this hold for} \quad z_*=z_h, \\ &b) \quad \mathcal{I}=0, \text{in our case is unstable} \end{aligned}$$

- **a)** $z_*=z_h$.

$$\begin{aligned} \frac{\ell}{2} &= PL^2\int_0^{z_h}\frac{\sqrt{2}e^{-2\mathcal{A}_s-c_Bz^2}\left(\frac{z}{L}\right)^{2/\nu}}{\sqrt{g(1-g)}}dz+\ldots \\ \frac{\mathcal{S}}{2} &= S_0+L^2P^2\int_0^{z_h}\frac{e^{-2\mathcal{A}_s(z)-c_Bz^2}\left(\frac{z}{L}\right)^{2/\nu}dz}{\sqrt{2g(1-g)}}+\ldots \end{aligned}$$

I. Y. Aref'eva, A. Hajilou, A. Nikolaev and P. S., PRD **112** (2025) 126007

Arbitrary orientation for JQ

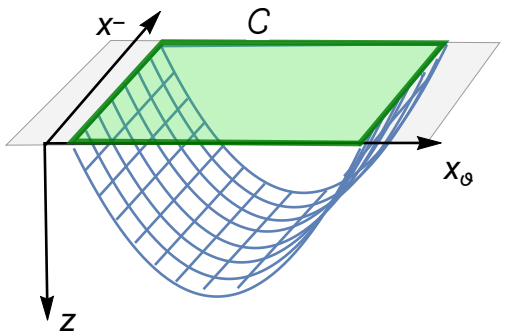

$$ds^2 = \frac{L^2 \mathfrak{b}_s(z)}{z^2}\left[-g(z)dt^2 + \mathfrak{g}_1 dx^2 + \mathfrak{g}_2 dy_1^2 + \mathfrak{g}_3 dy_2^2 + \frac{dz^2}{g(z)}\right],$$

$$\hat{q} = \frac{L^2}{\pi\alpha' a}, \qquad a = \frac{L^2 L^-}{2\sqrt{2}\pi\alpha'}\int_0^{z_h}\frac{dz}{\mathcal{F}(z)M(z)}.$$

$$x^- = \tau, \qquad x_j = \xi\sin\theta, \qquad x_k = \xi\cos\theta, \qquad x^+ = const, \qquad z = z(\xi),$$

$$i, j, k \quad \text{are distinct and} \quad i, j, k = 1, 2, 3$$

$$a_\theta = \int_0^{z_h}\frac{z^2 dz}{(\mathfrak{g}_j(z)sin^2\theta + \mathfrak{g}_k(z)cos^2\theta)\mathfrak{b}_s(z)\sqrt{(\mathfrak{g}_i(z) - g(z))g(z)}}$$

P.S., Mosc. Univ. Phys. Bull.'25

Spatial Wilson loops. Parametrization

To describe the nesting of the 2-dimensional world sheet in 5-dimensional spacetime we use

$$
\begin{aligned}
X^0(\xi) &= const, \\
X^i(\xi) &= \sum_{\alpha=1,2} a_{i\alpha}(\phi,\theta,\psi)\,\xi^\alpha, \qquad i=1,2,3, \\
X^4(\xi) &= z(\xi^1),
\end{aligned}
$$

x^i are spatial coordinates and $a_{ij}(\phi,\theta,\psi)$ are entries of the rotation matrix. Here ϕ is the angle between ζ^1-axis and the node line (N), θ is the angle between ζ^3 and x^3-axes, ψ is the angle between the node line N and x^1-axis.

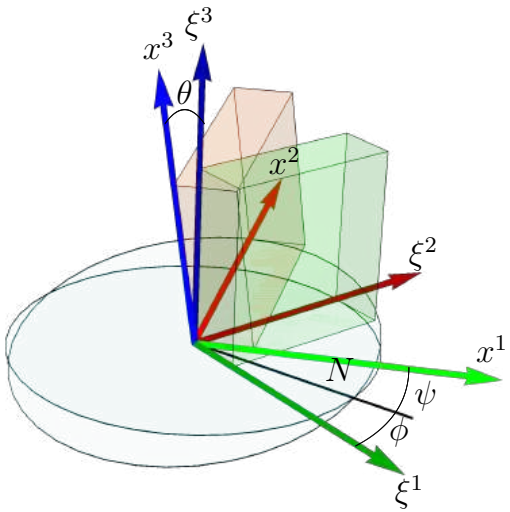

$$
\begin{aligned}
a_{11}(\phi,\theta,\psi) &= \cos\phi\cos\psi - \cos\theta\sin\phi\sin\psi, \\
a_{12}(\phi,\theta,\psi) &= -\cos\psi\sin\phi - \cos\phi\cos\theta\sin\psi, \\
a_{13}(\phi,\theta,\psi) &= \sin\theta\sin\psi, \\
a_{21}(\phi,\theta,\psi) &= \cos\theta\cos\psi\sin\phi + \cos\phi\sin\psi, \\
a_{22}(\phi,\theta,\psi) &= \cos\phi\cos\theta\cos\psi - \sin\phi\sin\psi, \\
a_{23}(\phi,\theta,\psi) &= -\cos\psi\sin\theta, \\
a_{31}(\phi,\theta,\psi) &= \sin\phi\sin\theta, \\
a_{32}(\phi,\theta,\psi) &= \cos\phi\sin\theta. \\
a_{33}(\phi,\theta,\psi) &= \cos\theta.
\end{aligned}
$$

Nambu-Goto action for Spatial Wilson Loop

Spatial Wilson loop (SWL):

$$\mathcal{S}_{SWL} = \int_{\mathcal{W}} \left(\frac{L^2 b_s}{z^2}\right) \sqrt{\left(\mathfrak{g}_1\mathfrak{g}_2 a_{33}^2 + \mathfrak{g}_1\mathfrak{g}_3 a_{23}^2 + \mathfrak{g}_2\mathfrak{g}_3 a_{13}^2 + \frac{z'^2}{g}\,\bar{g}_{22}\right)}\, d\xi^1 d\xi^2$$

$$\mathcal{V}_{SWL}(z) = \left(\frac{L^2 b_s}{z^2}\right) \sqrt{\mathfrak{g}_1\mathfrak{g}_2 a_{33}^2 + \mathfrak{g}_1\mathfrak{g}_3 a_{23}^2 + \mathfrak{g}_2\mathfrak{g}_3 a_{13}^2}$$

Holographic entanglement entropy (HEE):

$$\mathcal{S}_{HEE} = \int_{\mathcal{P}} \left(\frac{L^2 b_s}{z^2}\right)^{3/2} \sqrt{\left(\mathfrak{g}_1\mathfrak{g}_2\mathfrak{g}_3 + \frac{z'^2}{g}\,(\bar{g}_{22}\bar{g}_{33} - \bar{g}_{23}^2)\right)}\, d\xi^1 d\xi^2 d\xi^3,$$

$$\mathcal{V}_{HEE}(z) = \left(\frac{L^2 b_s}{z^2}\right)^{3/2} \sqrt{\mathfrak{g}_1\mathfrak{g}_2\mathfrak{g}_3},$$

g, $\mathfrak{g}_1$, $\mathfrak{g}_2$, $\mathfrak{g}_3$ are functions of z and $\bar{g}_{22}$, $\bar{g}_{33}$, $\bar{g}_{23}$ are functions of z and the Euler angles:

$$\begin{aligned}
\bar{g}_{22}(z,\phi,\theta,\psi) &= \mathfrak{g}_1 a_{12}^2 + \mathfrak{g}_2 a_{22}^2 + \mathfrak{g}_3 a_{32}^2,\\
\bar{g}_{33}(z,\phi,\theta,\psi) &= \mathfrak{g}_1 a_{13}^2 + \mathfrak{g}_2 a_{23}^2 + \mathfrak{g}_3 a_{33}^2,\\
\bar{g}_{23}(z,\phi,\theta,\psi) &= \mathfrak{g}_1 a_{12} a_{13} + \mathfrak{g}_2 a_{22} a_{23} + \mathfrak{g}_3 a_{32} a_{33}
\end{aligned}$$

I. Y. Aref'eva, A. Patrushev, P.S. JHEP **07**, 043 (2020)

Born-Infeld type action (1-dim dynamic model):

$$\mathcal{S} = \int_{-\ell/2}^{\ell/2} M(z(\xi))\sqrt{\mathcal{F}(z(\xi)) + (z'(\xi))^2}\, d\xi, \quad V(z(\xi)) = M(z(\xi))\sqrt{\mathcal{F}(z(\xi))}$$

We have two options to have $\ell \to \infty$ I. Aref'eva, EPJ Web Conf. **191**, 05010 (2018)

Born-Infeld type action. First option.

1) The existence of a stationary point of $\mathcal{V}(z)$ for $0 < z < z_h$: $\mathcal{V}'\Big|_{z_{DW}} = 0$.

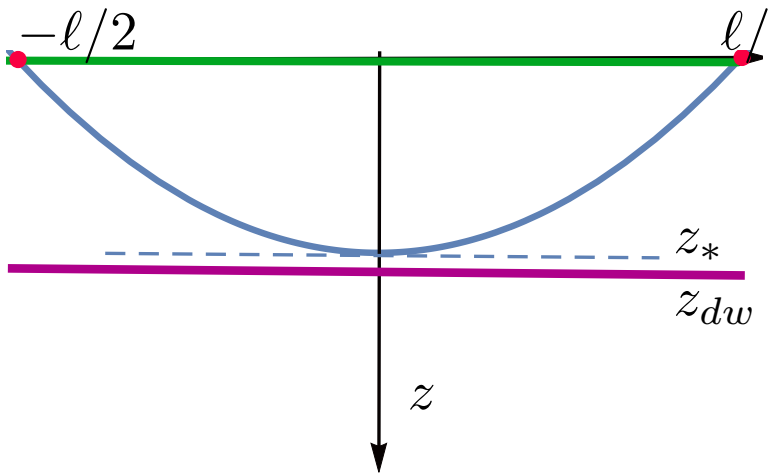

$$\ell \underset{z\to z_{DW}}{\sim} \frac{1}{\sqrt{F(z_{DW})}} \sqrt{\frac{\mathcal{V}(z_{DW})}{\mathcal{V}''(z_{DW})}}\, \log(z - z_{DW}),$$

$$\mathcal{S} \underset{z\to z_{DW}}{\sim} M(z_{DW}) \sqrt{\frac{\mathcal{V}(z_{DW})}{\mathcal{V}''(z_{DW})}}\, \log(z - z_{DW}).$$

$$\mathcal{S} \sim \sigma_{DW} \cdot \ell,$$

$$\sigma_{DW} = M(z_{DW}) \sqrt{F(z_{DW})}.$$

Born-Infeld type action. Second option.

2) There is no stationary point of $\mathcal{V}(z)$ in the region $0 < z < z_h$ and we suppose it to be near horizon

$$F(z) = \mathfrak{F}(z_h)(z_h - z) + \mathcal{O}((z_h - z)^2),$$

if $M(z) \underset{z \to z_h}{\to} \infty$ as

$$M(z) \underset{z \sim z_h}{\sim} \frac{\mathcal{M}(z_h)}{\sqrt{z - z_h}},$$

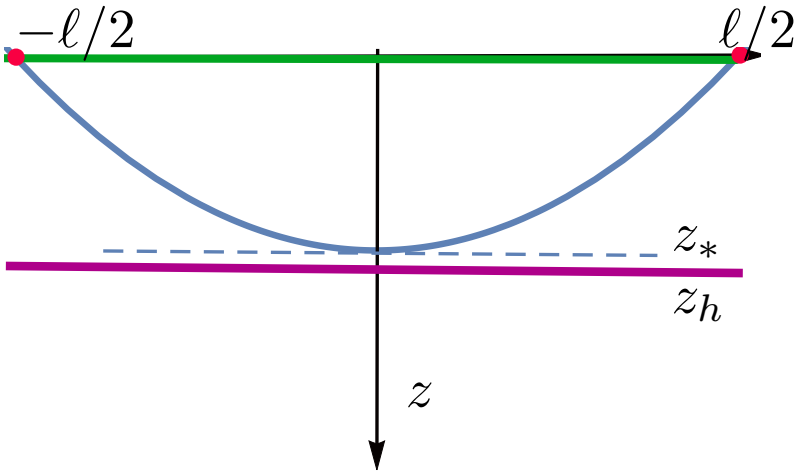

$$\ell \underset{z \to z_h}{\sim} \frac{1}{\sqrt{\mathfrak{F}(z_h)}} \frac{1}{\sqrt{-\frac{2\mathcal{V}'(z_h)}{\mathcal{V}(z_h)}}} \log(z - z_h),$$

$$\mathcal{S} \underset{z \to z_h}{\sim} \mathcal{M}(z_h) \frac{1}{\sqrt{-\frac{2\mathcal{V}'(z_h)}{\mathcal{V}(z_h)}}} \log(z - z_h).$$

$$\sigma_h = \mathcal{M}(z_h) \sqrt{\mathfrak{F}(z_h)} = M(z_h) \sqrt{F(z_h)}.$$

DW equations for SWLs

The equations for the DW for SWL in particular cases for different orientations:

$$xY_1 \text{ and } Xy_1: \quad \left.\frac{2b_s'(z)}{b_s(z)}+\frac{\mathfrak{g}_1'(z)}{\mathfrak{g}_1(z)}+\frac{\mathfrak{g}_2'(z)}{\mathfrak{g}_2(z)}-\frac{4}{z}\right|_{z=z_{DW}}=0,$$

$$xY_2: \quad \left.\frac{2b_s'(z)}{b_s(z)}+\frac{\mathfrak{g}_1'(z)}{\mathfrak{g}_1(z)}+\frac{\mathfrak{g}_3'(z)}{\mathfrak{g}_3(z)}-\frac{4}{z}\right|_{z=z_{DW}}=0,$$

$$y_1Y_2: \quad \left.\frac{2b_s'(z)}{b_s(z)}+\frac{\mathfrak{g}_2'(z)}{\mathfrak{g}_2(z)}+\frac{\mathfrak{g}_3'(z)}{\mathfrak{g}_3(z)}-\frac{4}{z}\right|_{z=z_{DW}}=0.$$

I Aref'eva, K. Rannu, P.S., TMPh, 206:3 (2021) [arXiv:2012.05758]